

## Role of oxygen vacancies in the flux-pinning mechanism, and hole-doping lattice disorder in high-current-density $\text{YBa}_2\text{Cu}_3\text{O}_{7-x}$ films

R. Feenstra, D. K. Christen, C. E. Klabunde, and J. D. Budai

*Solid State Division, Oak Ridge National Laboratory, Oak Ridge, Tennessee 37831-6057*

(Received 29 October 1991)

Critical-current measurements on epitaxial  $\text{YBa}_2\text{Cu}_3\text{O}_{7-x}$  films with  $0 \leq x \leq 0.2$  demonstrate that chain-site oxygen vacancies are not strong flux-pinning centers in high- $J_c$  films.  $J_c$  decreased steadily with increasing  $x$ , consistent with the predicted, monotonic dependence of pinning energy on mobile-charge-carrier density in strongly pinned systems. A correlation between the oxygen pressure  $p_{\text{O}_2}$  during high-temperature growth and subsequent response to low-temperature variation of  $x$  was observed for  $T_c$ . Specifically, films grown at low  $p_{\text{O}_2} = 0.00026$  atm appeared overdoped with holes after oxidation at  $p_{\text{O}_2} = 1.0$  atm, indicative of hole-doping defect formation at low initial oxygen contents.

A distinctive feature of  $\text{YBa}_2\text{Cu}_3\text{O}_{7-x}$  among other superconducting oxides is the large variable oxygen deficiency  $0 < x < 1$  tolerated by its lattice structure. The oxygen nonstoichiometry resides primarily on the Cu(1) basal plane, which ranges from being nearly half-filled with chains along the  $b$  axis, to nearly free of oxygen atoms.

Oxygen vacancies play a vital role in the synthesis of superconducting  $\text{YBa}_2\text{Cu}_3\text{O}_{7-x}$ . Primarily, the oxygen defects provide a variable and readily adjustable charge reservoir<sup>1,2</sup> for the superconducting  $[\text{Cu}(2)\text{O}_2]_\infty$  sheets, giving rise to the characteristic, two-plateau-like dependence of transition temperature  $T_c$  on chain-site oxygen occupancy and Cu(1)-O coordination,<sup>3</sup> with  $T_c \approx 92$  K after low-temperature ( $< 600^\circ\text{C}$ ) oxidation in 1.0 atm of oxygen ( $x \rightarrow 0$ ). On the other hand, large numbers of oxygen vacancies are present at high temperatures where they enhance the synthesis, apparently, by increasing cation diffusion rates.<sup>4,5</sup> Low-oxygen-pressure growth conditions for films (*in situ*<sup>6</sup> or *ex situ*<sup>7</sup>) may involve initial oxygen contents  $z \approx 7 - x$  less than 6.1.

The role of residual chain-site oxygen defects as effective pinning centers in  $\text{YBa}_2\text{Cu}_3\text{O}_{7-x}$  recently was discussed by Daeumling *et al.*,<sup>8</sup> following observations of enhanced flux-pinning and higher critical-current densities  $J_c$  in oxygen deficient single crystals with  $T_c \geq 90$  K. Evaluation of the pinning mechanism in high- $J_c$  films<sup>9</sup> also indicates a high density of small pinning defects with average spacings estimated on the order of 50 Å. These spacings are significantly less than those observed for planar defects in high-resolution electron microscopy, or the screw dislocations recently revealed by scanning tunneling microscopy,<sup>10</sup> suggesting that, if oxygen vacancies indeed represent strong pinning centers, further enhancement and optimization of critical currents should be possible by variation of the oxygen content.

In this paper, we report an integrated study of the role of oxygen vacancies in epitaxial  $\text{YBa}_2\text{Cu}_3\text{O}_{7-x}$  films that correlates the initial processing conditions (giving rise to different initial oxygen contents during growth) and the effects of small variations in residual oxygen deficiency  $x$

on superconducting properties ( $T_c$  and  $J_c$ ). It can be concluded that chain-site oxygen defects do not provide strong pinning sites in high-current-density films. Furthermore, it is found that even after full low-temperature oxygenation, effects of the initial oxygen composition remain, presumably, because of processing dependent cation disorder.

The  $\text{YBa}_2\text{Cu}_3\text{O}_{7-x}$  films were formed by  $e$ -beam coevaporation of Y,  $\text{BaF}_2$ , and Cu, followed by post-deposition annealing in controlled (wet)  $\text{Ar} + \text{O}_2$  ambients.<sup>7</sup> Although many combinations of annealing temperature and oxygen pressure were investigated, here we report on films annealed at  $835^\circ\text{C}/1.0$  atm (duration 0.5 h) and a second set annealed at  $800^\circ\text{C}/0.00026$  atm (duration 2 h; 1 h in wet and 1 h in dry ambients). For brevity we shall refer to these films as "high  $p_{\text{O}_2}$ " and "low  $p_{\text{O}_2}$ " films, respectively. Corresponding equilibrium<sup>11</sup> oxygen stoichiometries under these annealing conditions are  $\text{YBa}_2\text{Cu}_3\text{O}_{6.45}$  and  $\text{YBa}_2\text{Cu}_3\text{O}_{6.05}$ . Film thicknesses ranged from 230 to 260 nm, and (100)  $\text{SrTiO}_3$  was used as a substrate. The samples were cooled in dry  $p_{\text{O}_2}$  ambients to  $550^\circ\text{C}$  for a 0.5-h soak in 1.0 atm of oxygen prior to further slow cooling. Epitaxial films with the  $c$  axis perpendicular to the substrate were obtained with either anneal, as confirmed by x-ray diffraction on selected samples. Volume fractions of domains having the  $c$  axis parallel to the substrate were estimated to be  $< 2\%$ . The fully oxygenated  $c$  axis lengths were 11.67 Å, both for high  $p_{\text{O}_2}$  and low  $p_{\text{O}_2}$  films, i.e., slightly smaller than for single crystals<sup>2</sup> with  $z = 6.93$ . For transport  $J_c$  measurements, constrictions 40  $\mu\text{m}$  wide and 3 mm long, were patterned by standard photolithography. Silver or gold contact pads were sputter deposited and annealed for 1 h at  $550^\circ\text{C}$  in 1.0 atm of oxygen. The condition of the samples after this anneal was henceforth considered as the fully oxygenated starting condition. A 1  $\mu\text{V}/\text{cm}$  criterion was used for the  $J_c$  measurements.

Controlled variation of the residual oxygen deficiency resulted from successive, 1 h anneals at  $550^\circ\text{C}$  (followed by furnace cooling) in oxygen partial pressures  $0.01 \leq p_{\text{O}_2} \leq 1.0$  atm. Representative resistivity versus temperature curves are depicted in Fig. 1, showing a mono-

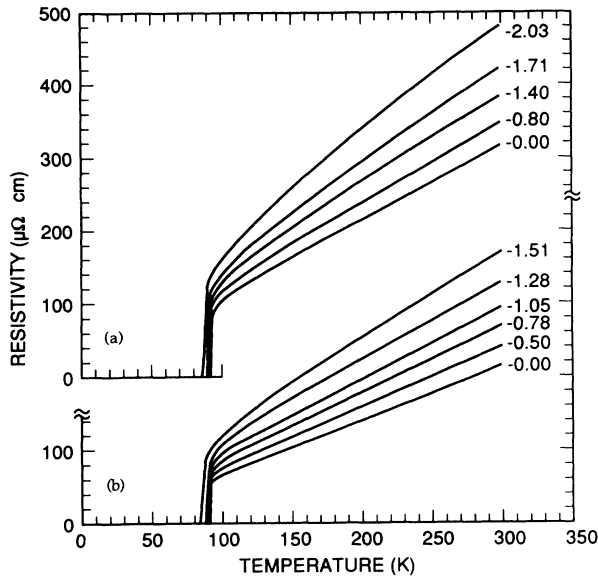


FIG. 1. Temperature dependence of normal-state resistivity for  $\text{YBa}_2\text{Cu}_3\text{O}_{7-x}$  films grown at (a)  $835^\circ\text{C}$ ,  $p_{\text{O}_2}=1.0$  atm, or (b)  $800^\circ\text{C}$ ,  $p_{\text{O}_2}=0.00026$  atm after successive anneals at  $550^\circ\text{C}$  and  $p_{\text{O}_2}\leq 1.0$  atm. The oxygen pressure is indicated as  $\log_{10}(p_{\text{O}_2}/\text{atm})$  for each curve.

tonic increase of the resistivity with decreasing  $p_{\text{O}_2}$ , both for high  $p_{\text{O}_2}$  and low  $p_{\text{O}_2}$  films.  $T_c$ , on the other hand, initially remained nearly unchanged at values close to 90 K, as expected for small  $x$ . The uppermost curve in either family marks the end of the 90 K plateau, giving rise to a sudden increase in transition width  $\Delta T_c$  from values  $< 1$  K to  $\Delta T_c > 3$  K. A comparison with bulk  $\text{YBa}_2\text{Cu}_3\text{O}_{7-x}$

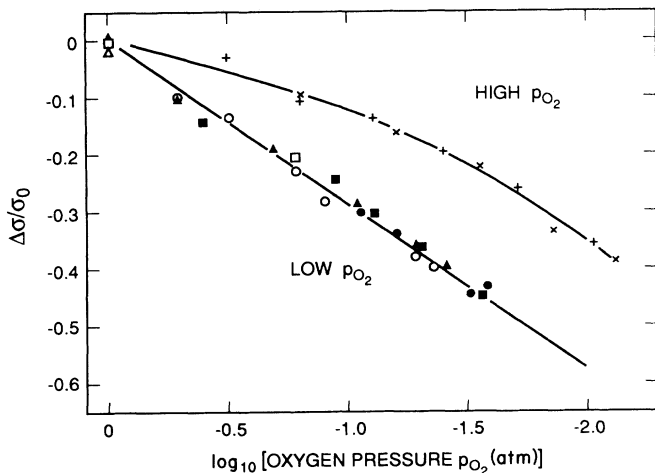


FIG. 2. Variation of the normalized change in conductivity  $\Delta\sigma/\sigma_0$  at 100 K in  $\text{YBa}_2\text{Cu}_3\text{O}_{7-x}$  films grown at  $835^\circ\text{C}$ ,  $p_{\text{O}_2}=1.0$  atm ("high  $p_{\text{O}_2}$ ") or at  $800^\circ\text{C}$ ,  $p_{\text{O}_2}=0.00026$  atm ("low  $p_{\text{O}_2}$ ") with oxygen pressure during successive oxidation anneals at  $550^\circ\text{C}$ . Filled and open symbols refer to data taken after decreasing or increasing oxygen pressure, respectively. The different symbols refer to different samples. By definition,  $\Delta\sigma/\sigma_0=0$  for the fully oxygenated starting condition after annealing in 1.0 atm oxygen.

suggests that  $z \approx 6.8$  for these curves.<sup>1-3</sup>

The change in electrical conductivity at 100 K is plotted in Fig. 2 as  $\Delta\sigma/\sigma_0 = [\sigma(p_{\text{O}_2}) - \sigma_0]/\sigma_0$ , i.e., relative to and normalized by the fully oxygenated starting condition. Good agreement was obtained for films having undergone the same initial heat treatment. As expected for chain-site oxygen exchange, the induced changes in normal state conductivity were essentially reversible.

The variations of  $T_c$  and  $J_c$  in zero applied magnetic field with residual oxygen deficiency are shown in Figs. 3(a) and 3(b), using  $\Delta\sigma/\sigma_0$  to parametrize the changing oxygen content. Remarkably, nonmonotonic  $T_c$  variations resulted for the low  $p_{\text{O}_2}$  films [Fig. 3(b)] with  $T_c$  rising from  $\sim 90$  K after oxidation at  $p_{\text{O}_2}=1.0$  atm to a maximum of  $\sim 92$  K after oxidation at  $p_{\text{O}_2}\approx 0.06$  atm. Simultaneously,  $J_c$  essentially decreased with increasing  $x$ , reaching its optimal value at low temperatures only after full oxygenation at  $p_{\text{O}_2}=1.0$  atm.<sup>12</sup> Thus, the maximum values of  $T_c$  and  $J_c$  could not be reached with one and the same oxidation anneal for films initially reacted at  $p_{\text{O}_2}=0.00026$  atm. Aging effects<sup>3</sup> due to oxygen ordering were not observed at these compositions.

By contrast, for the high  $p_{\text{O}_2}$  films both  $T_c$  and  $J_c$  maximized after oxidation in 1.0 atm of oxygen [Fig. 3(a)]. The plateaulike  $T_c$  variation resembles that observed for

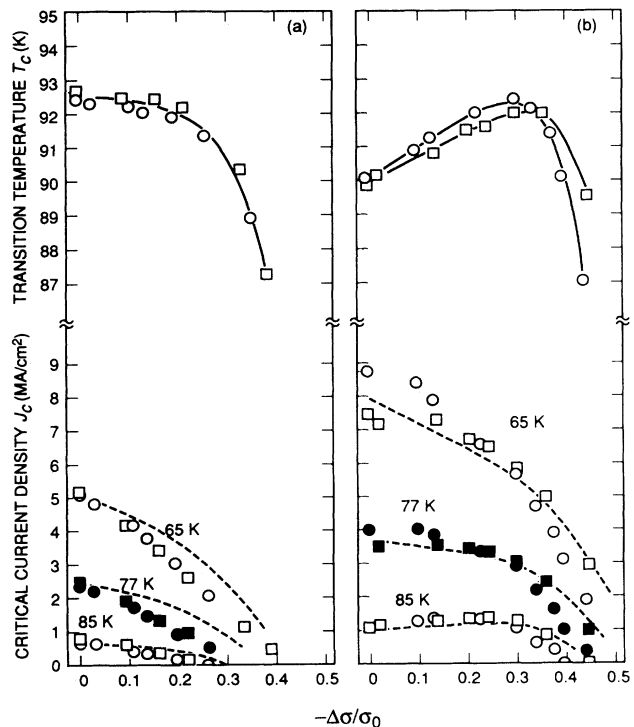


FIG. 3. Variation of midpoint transition temperature  $T_c$  and critical-current density  $J_c$  at 65, 77, and 85 K in self-field with normalized change in conductivity  $\Delta\sigma/\sigma_0$  for (a) two films grown at  $835^\circ\text{C}$ ,  $p_{\text{O}_2}=1.0$  atm, and (b) two films grown at  $800^\circ\text{C}$ ,  $p_{\text{O}_2}=0.00026$  atm. Different symbols were used for different samples. The solid lines ( $T_c$ ) are to guide the eye. The dashed lines ( $J_c$ ) represents a fit based on the near-optimal pinning model given by Eq. (2) for the samples indicated by squares.

bulk  $\text{YBa}_2\text{Cu}_3\text{O}_{7-x}$ .<sup>1-3</sup> Nearly linear scaling of  $J_c$  and  $\Delta\sigma/\sigma_0$  is observed at each indicated temperature; the curved  $J_c(x)$  dependences for the low  $p_{\text{O}_2}$  films evidently correlate with the initial rise in  $T_c$  occurring in the entire film. These results were systematic and reproducible and suggest the existence of electronically active, microstructural differences between films grown at different oxygen pressures, (meta)stable up to at least the oxidation temperature of 550°C.

The variation of  $J_c$  at 77 K with applied magnetic field  $H$  is shown in Figs. 4(a) and 4(b) for a high  $p_{\text{O}_2}$  and low  $p_{\text{O}_2}$  film, respectively, at oxygen stoichiometries obtained after oxygenation in either 1.0 atm of oxygen or at  $p_{\text{O}_2}=0.05$  atm. For the high  $p_{\text{O}_2}$  film, nearly equal transition temperatures  $T_c \approx 92$  K resulted after either oxidation anneal. For the low  $p_{\text{O}_2}$  film,  $T_c$  increased from 90.6 (1.0 atm) to 92.3 K (0.05 atm).

The usual anisotropy<sup>13</sup> with respect to field orientation was observed for both films, with nearly field-independent, oxygen-induced  $J_c$  reductions for  $H \parallel (a,b)$ . With  $H \parallel c$ ,  $J_c$  decreased more rapidly with  $H$  for the more oxygen deficient composition. In both orientations, the field was perpendicular to the current direction. Unlike  $\text{YBa}_2\text{Cu}_3\text{O}_{7-x}$  crystals, no "fishtail" effect due to field-induced suppression of superconductivity near oxygen vacancies<sup>8</sup> was observed, nor was a crossing of the  $J_c$  curves for different  $x$ . The pinning barrier energies  $U_0$  for  $H \parallel c$  at 77

K decreased upon oxygen removal. These barriers were derived in the limit of zero current density from the exponential variation of the thermally activated resistivity with  $1/B$  at fields above the "irreversibility" line.<sup>13</sup> For the sample of Fig. 4(a),  $U_0B$  decreased from 14500 to 9400 (in units Kelvin Tesla). For the low  $p_{\text{O}_2}$  film of Fig. 4(b),  $U_0B$  decreased from 13300 to 8500, implying weaker pinning for both films with increasing oxygen deficiency.

A direct dependence of  $J_c$  on mobile-charge-carrier density can be derived in the limit of very strong flux pinning. For extended defects that pin well-separated vortices over their entire lengths (near-optimal pinning), one obtains for a maximum critical current density,<sup>14</sup>

$$J_c^{\text{max}} \approx \frac{cu_0}{\phi_0 \xi_{ab}} = \frac{c\phi_0}{64\pi^2 \lambda_{ab}^2 \xi_{ab}}, \quad (1)$$

where  $u_0 = [H_c^2/8\pi] \pi \xi_{ab}^2$  is the pinning energy per unit length of an optimal linear defect,  $H_c$  is the thermodynamic critical field,  $\phi_0$  the magnetic flux quantum, and  $\xi_{ab}$  and  $\lambda_{ab}$  are the basal-plane superconducting coherence length and magnetic penetration depth, respectively. Estimates of  $J_c^{\text{max}}$  exceed the measured values by only a factor of 2-3, indicative of the strong pinning in high- $J_c$  films. From Eq. (1), the clean-limit results  $\lambda^{-2} \propto n_s$  and  $\xi(T=0) \propto T_c^{-1}$  yield  $J_c^{\text{max}} \propto n_s(T=0) T_c (1 - T/T_c)^{3/2}$ . If one further assumes that the pair carrier density  $n_s$  is linearly related to the mobile hole density  $n_h$ , then a Drude normal-state conductivity leads to the expected, implicit dependent on oxygen content  $x$ ,

$$\frac{J_c(x)}{J_c(0)} = \left[ 1 - \frac{\Delta\sigma(x)/\sigma_0}{\Delta\sigma_{J_c,0}/\sigma_0} \right] \frac{T_c(x)}{T_c(0)} \left[ \frac{1 - T/T_c(x)}{1 - T/T_c(0)} \right]^{3/2}. \quad (2)$$

In Eq. (2), we have allowed for a normalization that accounts for the observed disappearance of  $J_c$  at a finite conductivity, i.e.,  $J_c(T=0) \rightarrow 0$  near  $\Delta\sigma_{J_c,0}/\sigma_0 \approx -0.78$ . The results of Eq. (2) are plotted as dashed lines in Fig. 3, using the  $T_c$  data for one of each film type ( $\square$ ). The overall agreement is acceptable; deviations may be ascribed to carrier density effects on the Fermi velocity (occurring in  $\xi_{ab}$ ), inequivalence of  $n_s$  and  $n_h$ , changes in carrier lifetime, or effects of thermally activated flux motion.

The following picture emerges from this analysis. In strongly pinned systems such as  $\text{YBa}_2\text{Cu}_3\text{O}_{7-x}$  thin films, reduction of the mobile-charge-carrier density by oxygen removal decreases  $J_c$  by diminishing the pinning strengths of all pre-existing pinning centers. In crystals, because of fewer or weaker pre-existing pinning defects, apparently the positive effect of added pinning centers at oxygen vacancies overcompensates the electronic reduction of pinning energies, giving rise to higher  $J_c$  values at small oxygen deficiencies.<sup>8</sup> The overall  $J_c$  level, however, is much lower than in films, suggesting only weak pinning by the additional oxygen defects. The different effects in films and crystals, therefore, are not contradictory, but reflect different numbers of naturally occurring, strong-pinning defects (other than chain-site oxygen vacancies) in either material. In related work, this view recently was corro-

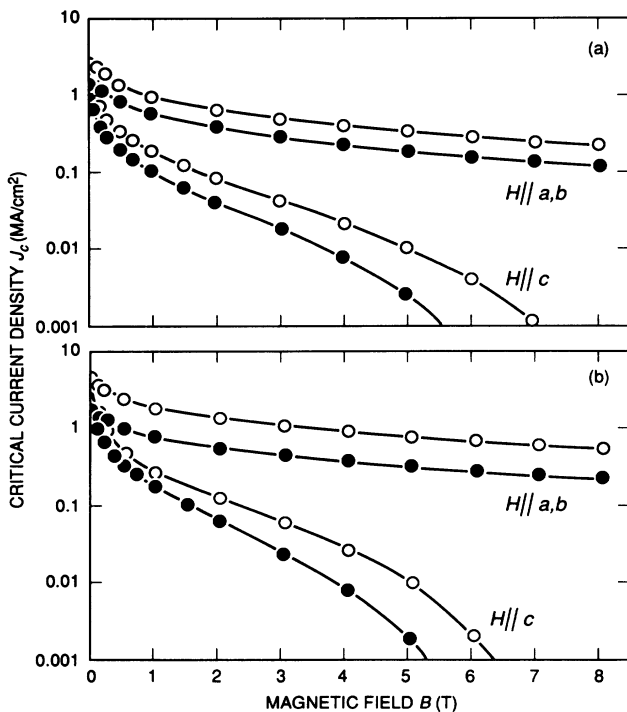


FIG. 4. Magnetic-field dependence of critical-current density  $J_c$  at 77 K for (a) a high  $p_{\text{O}_2}$  film grown at 835°C,  $p_{\text{O}_2}=1.0$  atm, and (b) a low  $p_{\text{O}_2}$  film grown at 800°C,  $p_{\text{O}_2}=0.00026$  atm. Open symbols: fully oxygenated compositions after oxidation at  $p_{\text{O}_2}=1.0$  atm. Filled symbols: oxygen deficient compositions after oxidation at  $p_{\text{O}_2}=0.05$  atm. The field orientations are indicated in the figure.

borated by magnetic studies on aligned polycrystalline  $\text{YBa}_2\text{Cu}_3\text{O}_{7-x}$ .<sup>15</sup>

Regarding the  $T_c$  response to residual oxygen deficiency, the observed additional dependence on preparation history indicates the presence of growth related, charged lattice defects, probed by the variation of carrier density upon chain-site oxygen exchange. Taken at face value, the nonmonotonic  $T_c(x)$  dependences of the low  $p_{\text{O}_2}$  films resemble those observed<sup>16</sup> for the extrinsically doped system  $(\text{Y}_{1-y}\text{Ca}_y)\text{Ba}_2\text{Cu}_3\text{O}_{7-x}$  and, indeed, universally for oxide superconductors with changing charge-carrier density. In the Ca-doped system, divalent Ca substitutes for trivalent Y, adding one hole per Ca atom to the electronic system compared to undoped  $\text{YBa}_2\text{Cu}_3\text{O}_{7-x}$ . The optimum  $T_c$  value then requires fewer holes from the oxygen atoms, i.e., a lower oxygen content.

Based on this analogy and the acknowledged influence of oxygen pressure on growth properties,<sup>4-7</sup> the peaked  $T_c(x)$  dependences of Fig. 3(b) should be attributed, most likely, to hole-doping cation disorder on the charge reservoir layers. As one possible candidate we mention Ba disorder on the Y site, recently proposed (on different grounds) by Matijasevic *et al.*<sup>17</sup> for  $\text{YBa}_2\text{Cu}_3\text{O}_{7-x}$  films grown *in situ* at very low  $p_{\text{O}_2}$  ( $< 10$  mTorr). Similar to these *in situ* films, the low  $p_{\text{O}_2}$  postannealed films of our study were crystallized under conditions close to the  $\text{YBa}_2\text{Cu}_3\text{O}_{7-x}$  stability limit at low oxygen contents.<sup>18</sup> Ba(Y) disorder could be thermodynamically driven under those conditions. Possible other causes for the processing dependent  $T_c(x)$  variations are systematic differences in oxidation-induced strain in the films, oxygen vacancy ordering, or other types of cation disorder.

In summary, a systematic, correlative study of superconducting properties, oxygen deficiency, and initial processing conditions was carried out for  $\text{YBa}_2\text{Cu}_3\text{O}_{7-x}$  thin films. Films were grown at different initial oxygen pressures (1.0 or 0.00026 atm) and subsequently annealed at low temperatures and oxygen pressures between 1.0 and 0.01 atm to produce reversible changes in residual oxygen deficiency and carrier density on the superconducting  $[\text{CuO}_2]_{\infty}$  planes. The two principle conclusions are the following:

(i) Reduction of the mobile-charge-carrier density by oxygen removal diminishes the pinning energies of strong flux-pinning centers, giving rise to significant  $J_c$  reductions in oxygen deficient films, even for oxygen compositions where  $T_c \geq 90$  K. Thus, chain-site oxygen vacancies are not strong pinning centers in high- $J_c$  films.

(ii) The variation of carrier density upon low-temperature oxygen exchange, apparently, is capable of detecting subtle microstructural differences that give rise to additional charge transfer. Here, different defect structures presumably originated from initial-oxygen-content-dependent growth properties. The resulting peaked  $T_c(x)$  variations for films grown at low  $p_{\text{O}_2}$  signal the presence of hole doping lattice disorder that is absent in films grown at  $p_{\text{O}_2} = 1.0$  atm.

The authors wish to thank P. H. Fleming for film patterning and acknowledge valuable discussions with J. G. Ossandon and J. R. Thompson. This research was sponsored by the Division of Materials Science, U.S. Department of Energy under Contract No. DE-AC05-84OR21400 with Martin Marietta Energy Systems, Inc.

<sup>1</sup>R. J. Cava *et al.*, *Physica C* **165**, 419 (1990).

<sup>2</sup>J. D. Jorgensen *et al.*, *Phys. Rev. Lett.* **B 41**, 1863 (1990).

<sup>3</sup>B. W. Veal *et al.*, *Phys. Rev. B* **42**, 6305 (1990).

<sup>4</sup>N. Chen *et al.*, *J. Appl. Phys.* **66**, 2485 (1989).

<sup>5</sup>J. L. Routbort *et al.*, *Phys. Rev. B* **43**, 5489 (1991).

<sup>6</sup>R. H. Hammond and R. Bormann, *Physica C* **162-164**, 703 (1989).

<sup>7</sup>R. Feenstra *et al.*, *J. Appl. Phys.* **69**, 6569 (1991).

<sup>8</sup>M. Daeumling *et al.*, *Nature (London)* **346**, 332 (1990).

<sup>9</sup>T. L. Hylton and M. R. Beasley, *Phys. Rev. B* **41**, 11669 (1990).

<sup>10</sup>C. Gerber *et al.*, *Nature (London)* **350**, 279 (1991); M. Haw-

ley *et al.*, *Science* **251**, 1587 (1991).

<sup>11</sup>T. B. Lindemer *et al.*, *J. Am. Ceram. Soc.* **72**, 1775 (1989).

<sup>12</sup>Since the actual oxygen content in the films is unknown, it is possible that  $x > 0$  and that higher  $J_c$  is obtained after oxidation at  $p_{\text{O}_2} > 1.0$  atm.

<sup>13</sup>D. K. Christen *et al.*, *Mater. Res. Soc. Symp. Proc.* **169**, 883 (1990).

<sup>14</sup>L. Civale *et al.*, *Phys. Rev. Lett.* **67**, 648 (1991).

<sup>15</sup>J. G. Ossandon *et al.*, *Phys. Rev. B* (to be published).

<sup>16</sup>Y. Tokura *et al.*, *Phys. Rev. B* **38**, 7156 (1988).

<sup>17</sup>V. Matijasevic *et al.*, *J. Mater. Res.* **6**, 682 (1991).

<sup>18</sup>T. B. Lindemer *et al.*, *Physica C* **178**, 93 (1991).